Micelle-Assisted Synthesis of Quantum Dot Arrays. A Nanoreactor Approach for ZnO and ZnS Nanoparticles

Mourtas Spyridon [1*]

Abstract

Background. Quantum dots (QDs) are nanoscale semiconductor particles with unique optical and electronic properties, making them suitable for biomedical imaging, drug delivery, and biosensing applications. However, controlling their size and stability in physiological environments remains a challenge. This study investigated the use of polymeric micelles to encapsulate QDs and synthesize ZnO and ZnS nanoparticles to form nanoparticle arrays for biofunctionalization purposes. Methods. Micelle solutions were prepared using polystyrene-b-poly(2-vinylpyridine) (PS-b-P2VP) block copolymers. ZnO and ZnS nanoparticles were synthesized in situ by loading zinc precursors (ZnAc, $ZnCl_2$) into the micelles, followed by oxidation using tetramethylammonium hydroxide (TMA-OH) and sodium oxide (Na_2O). The nanoparticles were characterized by Dynamic Light Scattering (DLS), Scanning Electron Microscopy (SEM), and UV-Vis spectroscopy. Results. Uniform micelles with sizes ranging from 70-120 nm were successfully formed. ZnO nanoparticles (50-80 nm) displayed strong UV absorption at 370 nm, confirming the synthesis. ZnS nanoparticles (60 nm) were synthesized using $Na_2S•9H_2O$, exhibiting a UV absorption peak at 290 nm. Ex situ synthesis on silicon substrates using oxygen plasma produced well-ordered nanoparticle arrays. Conclusion. Polymeric micelles effectively served as nanoreactors for ZnO and ZnS nanoparticle synthesis. The choice of zinc precursor and oxidizing agent influenced particle size and uniformity. Ex situ techniques demonstrated potential for nanopatterning applications. Future work could focus on scaling up and adapting this method to other metal oxide and sulfide systems for advanced material design.

Keywords: Quantum Dots, Peptides, ZnO Nanoparticles, ZnS Nanoparticles, Micelle Synthesis

Significance | This study determined nanoparticle synthesis via micelles for biofunctionalization, optimizing conditions for stable quantum dot arrays.

*Correspondence. Mourtas Spyridon, University of Patras, Greece.
E-mail: mourtas@upatras.gr

Editor Muhit Rana, Ph.D., And accepted by the Editorial Board Dec 20, 2022 (received for review Oct 04, 2022)

1. Introduction

A quantum dot (QD) is a nanoscale semiconductor particle, typically ranging from 2 to 10 nm in size, whose excitons are confined in all three spatial dimensions. This confinement gives QDs unique optical and electronic properties that resemble the behavior of individual atoms, which result from the size-dependent quantum confinement effect (Wikipedia contributors, 2012). These properties place QDs between bulk semiconductors and discrete molecules, making them valuable in various applications, including biology, bioanalytics, and optoelectronics (Gao et al., 2004). Among these properties, QDs exhibit broad absorption spectra, narrow and tunable emission, high luminescence, long lifetimes, and resistance to photobleaching, making them highly desirable for biomedical imaging, diagnostics, and therapeutic applications (Alivisatos, 2004

Author Affiliation.
[1] University of Patras, Greece.

Please cite this article:
Mourtas Spyridon (2024). Micelle-Assisted Synthesis of Quantum Dot Arrays. A Nanoreactor Approach for ZnO and ZnS Nanoparticles, Biosensors and Nanotheranostics, 1(1), 1-7, 9897

; Wang et al., 2006). Quantum dots can be synthesized from various semiconductor materials, such as cadmium selenide (CdSe), cadmium sulfide (CdS), and zinc sulfide (ZnS), as well as from metallic and organic nanomaterials (Hines & Guyot-Sionnest, 1996; Murray et al., 1993). Each material offers distinct advantages in terms of optical properties and stability, with CdSe QDs being among the most studied due to their strong luminescence and ease of synthesis (Qu & Peng, 2002; Skaff & Emrick, 2003). Advances in synthetic methods have enabled researchers to control the size, shape, and surface chemistry of QDs, which is critical for optimizing their performance in specific applications (Murray et al., 1993).

The encapsulation of QDs in polymers, particularly block copolymers, has enabled the creation of stable, water-soluble QDs that retain their optical properties in various environments (Wu et al., 2009). For instance, stearyl methacrylate/methylacrylate copolymers have been used to enhance the stability and optical properties of CdSe/ZnS QDs, making them suitable for biological applications (Wu et al., 2009). This approach mitigates the challenges of QD aggregation and degradation under physiological conditions, which is essential for their use in imaging and therapeutic delivery systems (Song et al., 2011).

Recent research has focused on the preparation and functionalization of QD arrays using micellar lithography and self-assembly techniques (Tomczak et al., 2009; El-Atwani et al., 2010). These methods allow for precise control over QD placement and spacing, which is crucial for developing nanostructured devices and sensors. For example, micellar lithography has been employed to create ZnO and ZnS nanoparticle arrays that exhibit strong optical and electronic properties, useful in optoelectronics and photocatalysis (Chen et al., 2010; Hines & Guyot-Sionnest, 1996).

In biomedical applications, QDs have demonstrated remarkable potential for in vivo imaging, targeted drug delivery, and biosensing (Anikeeva et al., 2006; Gao et al., 2004). Their bright, tunable fluorescence allows for high-resolution imaging of cellular processes and disease markers, while their surface can be functionalized with peptides, proteins, or DNA for specific molecular targeting (Arnold et al., 2004). Furthermore, the ability to conjugate QDs with biological molecules enables the development of advanced diagnostic tools, such as biosensors that can detect low concentrations of pathogens or biomarkers (Zhou & Ghosh, 2006).

One of the major challenges in QD research is overcoming the potential toxicity associated with heavy metal content, particularly in Cd-based QDs (Farzaneh & Hamedani, 2006). Researchers have explored alternative materials, such as ZnO and silicon-based QDs, which offer similar optical properties without the associated health risks (Chen et al., 2010; Wang et al., 2006). Additionally, surface modifications and encapsulation strategies have been developed to reduce the release of toxic ions and improve the biocompatibility of QDs for medical applications (Zhao et al., 2001).

In conclusion, quantum dots represent a versatile and powerful tool for a wide range of applications, from optoelectronics to biomedicine. Advances in synthetic techniques, functionalization strategies, and safety profiles continue to expand their potential uses, paving the way for novel technological innovations in fields such as bioimaging, targeted therapy, and environmental sensing (Moffitt & Eisenberg, 1995; Skaff et al., 2002). The future of QD research lies in addressing challenges related to toxicity, scalability, and long-term stability, while exploring new materials and methods to further enhance their capabilities (Nanda et al., 2000; Zhou & Ghosh, 2006).

This research aims to form micelle solutions using polymers of different molecular weightsto control and vary the sizes of micelles. These micelles are used to encapsulate commercially available CdSe/ZnS quantum dots (QDs) for array formation. Additionally, the project involves synthesizing ZnO and ZnS nanoparticles within the micelles using metallic precursors. The final objective is to form nanoparticle arrays of CdSe/ZnS, ZnO, and ZnS QDs for biofunctionalization purposes.

2. Materials and Methods

2.1 Synthesis of Polymer Micelle Solutions

Polymeric micelle solutions were prepared by dissolving two diblock copolymers, polystyrene- b-poly(2-vinylpyridine) (PS-b-P2VP), in selective solvents. The polymers used were PS (110,000)-b-P2VP (52,000) and PS (52,100)-b-P2VP (31,000), each with polydispersity indices of 1.10 and 1.05, respectively. PS-b-P2VP was dissolved in toluene and para-xylene, solvents selective for the polystyrene (PS) blocks, at a concentration of 5 mg/mL (25 mg polymer in 5 mL solvent). The solutions were stirred at room temperature for at least 12 hours, exceeding the critical micelle concentration under ambient conditions.

2.2 In Situ Synthesis of ZnO Quantum Dots (QDs)

Zinc oxide (ZnO) nanoparticles were synthesized in situ by loading zinc salts into the prepared micelle solutions. Two zinc sources, zinc acetate (ZnAc) and zinc chloride ($ZnCl_2$), were tested. ZnAc was dissolved in propanol and stirred at 65°C for 90 minutes, while $ZnCl_2$ was dissolved in either propanol or anhydrous methanol at room temperature. The zinc salts were loaded into the micellar solutions at various Zn-to-pyridine unit ratios (ZnAc/VP. 0.3, 0.4, 0.5, 0.7, and 1.0), corresponding to 4.2, 5.6, 7.0, 9.8, and 14 mg of ZnAc, respectively. These were predissolved in 0.5 mL of propanol before being added to the micelle solutions, followed by stirring for 30 hours to achieve complete ion loading.

2.3 Formation of ZnO Nanoparticles

To form ZnO nanoparticles, two oxidizing agents were tested. tetramethylammonium hydroxide (TMA-OH) and sodium oxide

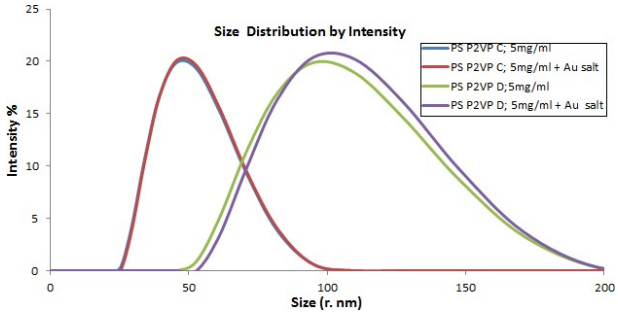

Figure 1. DLS intensity distribution of PS (110000)-b- P2VP (52000) (PS P2VP D) and PS (52100)-b- P2VP (31000) (PS P2VP C) micelle solution of xylene (5mg/ml concentration) loaded Au.

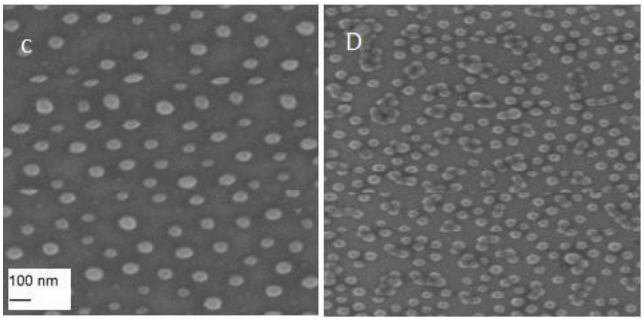

Figure 2. SEM image of Si-wafers structured with Au- loaded micelles of; (C) Polymer PS (110000)-b- P2VP (52000)in xylene and, (D) Polymer PS (52100)-b- P2VP (31000)in xylene

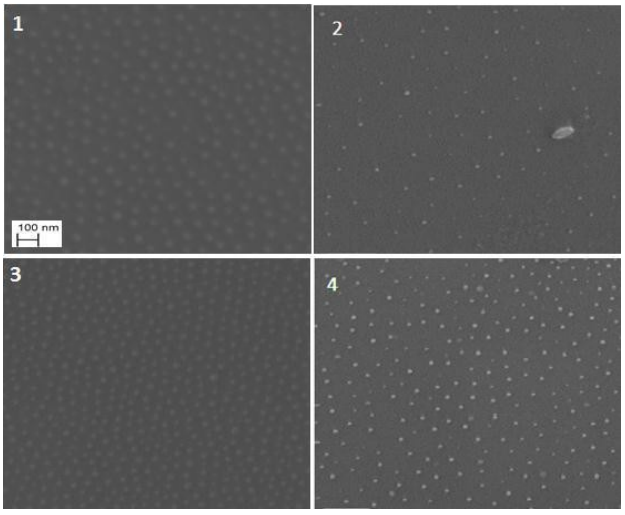

Figure 4. SEM image of Si-wafers structured with Zn2+ loaded micelles and ZnO nanodots before and after oxygen plasma treatment at two different loadings of; (1) 0.5 ZnAc in polymer PS (110000)-b- P2VP (52000) in xylene solution, (2) ZnO nanoparticle array formed at 0.5 ZnAc loading after treatment with oxygen plasma, (3) 0.3 ZnAc in polymer PS (110000)-b- P2VP (52000) in xylene solution, (4) ZnO nanoparticle array formed at 0.3 ZnAc loading after treatment with oxygen plasma.

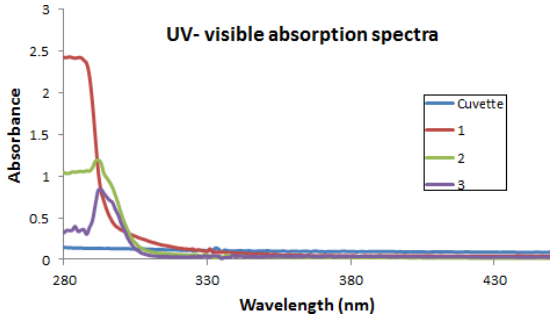

Figure 3. UV- VIS absorption spectra of elements before oxidation and sulfidation of zinc loaded micelles to form ZnO and ZnS particles; Cuvette. quartz cuvette, **(1)**. is a mixture of xylene and propanol (9.1) which is the composition of the solvent in the loaded micelle solution, **(2)**. xylene micelle solution of polymer D with propanol (9.1) and **(3)**. xylene micelle solution of polymer D loaded with ZnAc in propanol.

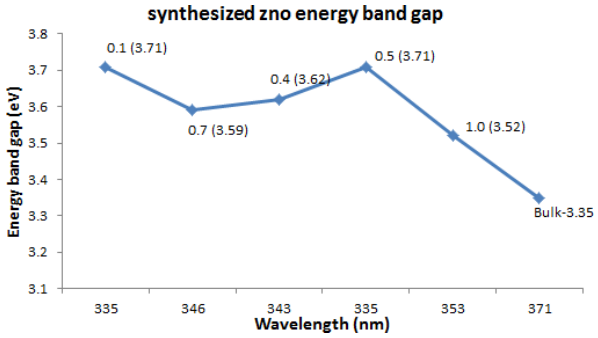

Figure 6. Plot of energy band of synthesized ZnO nanoparticles (at their corresponding loadings in bracket) against their wave length compared with the bulk ZnO particle showing a blue-shift in band gap energy.

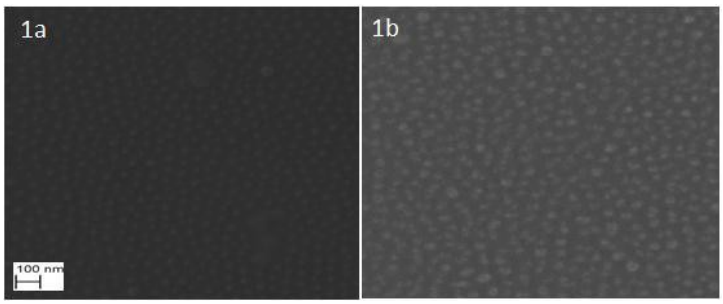

Figure 7. SEM image of Si-wafers structured with ZnS nanoparticles inside polymer micelles after sulfidization of 0.5 ZnAc loaded micelle solutions with H2S. (1a) and, (1b) were synthesized at different times and imaged at different times.

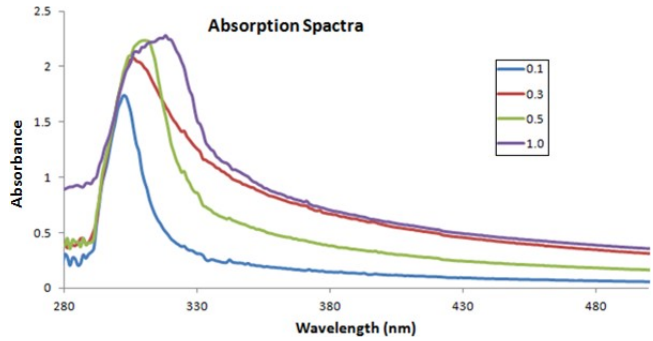

Figure 8. UV- vis absorption spectra of ZnS synthesis at various ratios of Zn2+/ VP loadings after bubbling with H2S for 40 minutes from the reaction of Na2S with water solution of nitric acid.

(Na_2O). TMA-OH (10 wt% in methanol) was first added to an empty micelle solution, then combined with the ZnAc-loaded micelles. The solution was stirred for an additional 24 hours. The amount of TMA-OH used was in excess (40 µL/mL), calculated based on the reaction.

2.4 nZnAc2+2nTMA-OH→nZnO+2nTMA-Ac+nH2O

Similarly, Na_2O (5 wt% in anhydrous methanol) was tested as an oxidizing agent, also used in excess (40 µL/mL) to ensure complete reaction of ZnAc. The process was repeated for $ZnCl_2$, using the same oxidizing agents, with $ZnCl_2$-to-oxidizer molar ratios calculated based on the following reactions.

2.5 nZnCl2+2nTMA-OH→nZnO+2nTMA-Cl+nH2O

The ZnO nanoparticles were deposited onto a silicon substrate, and the micellar shells were removed using oxygen plasma, hydrogen plasma, or ozone exposure, leaving behind an array of ZnO nanoparticles.

3.Results

3.1 Micelle Formation and Characterization

The polymer micelles were successfully formed by dissolving PS-b-P2VP in selective solvents (toluene and para-xylene). Dynamic Light Scattering (DLS) analysis confirmed the formation of micelles, with sizes ranging between 70 and 120 nm depending on the polymer concentration and solvent used (Figureure 1). The polydispersity index (PDI) of the micelles was low, indicating a narrow size distribution. Scanning Electron Microscope (SEM) images further validated the spherical morphology of the micelles (Figureure 2). The unloaded micelles displayed a smooth surface, while the zinc-loaded micelles exhibited distinct structural changes, confirming successful Zn^{2+} encapsulation.

3.2 In Situ Synthesis of ZnO Nanoparticles

The in situ synthesis of ZnO nanoparticles within the micelles was confirmed by SEM and UV- Vis spectroscopy (Figureure 3). SEM images showed a well-distributed array of nanoparticles with an average size of 50–80 nm (Figureure 4). The UV-Vis absorption spectra revealed a strong peak at 370 nm, corresponding to the characteristic absorbance of ZnO nanoparticles (Figureure 5). The energy band gap, calculated from the absorption peak using the equation E=hc/λE = hc/\lambdaE=hc/λ, was approximately 3.35 eV, consistent with the known band gap for ZnO.

The effect of different zinc precursors (ZnAc and $ZnCl_2$) and oxidizing agents (TMA-OH and Na_2O) on nanoparticle formation was investigated. Zinc acetate yielded smaller and more uniform ZnO particles compared to zinc chloride, as evidenced by the narrower size distribution observed in both SEM images and DLS measurements.

3.3 Ex Situ Synthesis of ZnO Nanoparticles

Ex situ synthesis using oxygen plasma on silicon substrates produced ZnO nanoparticle arrays with a higher degree of order and uniformity. SEM images revealed well-patterned arrays with particle sizes ranging from 30–50 nm. The oxygen plasma treatment not only etched away the micelle shells but also oxidized the encapsulated zinc ions into ZnO nanoparticles, as confirmed by energy-dispersive X-ray spectroscopy (EDS) analysis (Figureure 6).

3.4 Synthesis of ZnS Nanoparticles

The synthesis of ZnS nanoparticles using H_2S gas generated from sodium sulfide nonahydrate ($Na_2S•9H_2O$) in a custom-designed apparatus was successful. SEM images showed well- formed ZnS nanoparticles with an average size of 60 nm (Figureure 7). The UV-Vis absorption spectra exhibited a distinct peak at 290 nm, indicating the presence of ZnS nanocrystals (Figureure 8). The use of Na_2S as the sulfur source produced more uniform ZnS particles compared to potassium sulfide (K_2S).

4.Discussion

The results demonstrate that PS-b-P2VP micelles can effectively serve as nanoreactors for the synthesis of ZnO and ZnS nanoparticles. The successful formation of micelles was confirmed through DLS and SEM, which showed uniform spherical structures. The encapsulation of Zn^{2+} ions within the micelles allowed for controlled nanoparticle synthesis, as observed in both in situ and ex situ ZnO formation. The choice of zinc precursor and oxidizing agent had a significant impact on the size and uniformity of the nanoparticles, with zinc acetate and TMA- OH producing smaller, more uniform particles compared to zinc chloride and Na_2O.

The ex situ synthesis using oxygen plasma demonstrated the potential for patterning ZnO nanoparticles on silicon substrates. This approach not only allowed for the precise deposition of nanoparticles but also avoided the need for additional chemical oxidants, making it a more environmentally friendly process. The highly ordered arrays observed in SEM images suggest that this method could be useful for applications requiring nanopatterned surfaces, such as in optoelectronics and sensor technologies.

The ZnS nanoparticle synthesis using H_2S gas generated from $Na_2S•9H_2O$ was successful, providing a safer alternative to handling H_2S gas directly. The resulting ZnS particles were uniform in size and showed good optical properties, as evidenced by the UV-Vis spectra. This method could be further optimized for the synthesis of other metal sulfide nanoparticles by adjusting the reaction conditions, such as the concentration of the zinc precursor or the duration of the reaction.

Overall, the results support the use of polymeric micelles as versatile nanoreactors for the synthesis of metal oxide and sulfide nanoparticles. This method offers precise control over nanoparticle size and distribution and can be adapted for both in situ and ex situ syntheses.

5. Conclusion

This research highlights the successful synthesis of ZnO and ZnS nanoparticles within micellar nanoreactors formed by PS-b-P2VP polymers. The encapsulation of Zn^{2+} ions in these micelles facilitated controlled nanoparticle synthesis. Zinc acetate, coupled with TMA-OH, produced smaller and more uniform ZnO particles compared to zinc chloride and Na_2O. The ex situ method using oxygen plasma on silicon substrates generated highly ordered ZnO arrays, indicating the method's potential for nanostructured applications such as optoelectronics and sensor technologies. For ZnS synthesis, $Na_2S•9H_2O$ provided a safer, effective alternative for generating ZnS nanoparticles with uniformity and excellent optical properties. These findings suggest that micelle-assisted methods offer a scalable, environmentally friendly solution for synthesizing metal oxide and sulfide nanoparticles. Future research could investigate further optimization for industrial applications and explore the integration of other nanoparticle systems within this framework to develop advanced materials.

Author contributions

M.S. was responsible for the conceptualization and design of the study, contributed to the data analysis, and was actively involved in manuscript drafting and revisions. All authors have reviewed and approved the final manuscript.

Acknowledgment

Author would be like to thankful to their department.

Competing financial interests

The authors have no conflict of interest.

References

Alivisatos, P. (2004). The use of nanocrystals in biological detection. Nature Biotechnology, 22(1), 47–52.

Anikeeva, N., Lebedeva, T., Clapp, A. R., Goldman, E. R., Dustin, M. L., Mattoussi, H., & Sykulev, Y. (2006). Quantum dot/peptide-MHC biosensors reveal strong CD8-dependent cooperation between self and viral antigens that augment the T cell response. Proceedings of the National Academy of Sciences, 103(45), 16846–16851.

Arnold, M., Cavalcanti-Adam, E. A., Glass, R., Blümmel, J., Eck, W., & Kantlehner, M., et al. (2004). Activation of integrin function by nanopatterned adhesive interfaces. ChemPhysChem, 5(3), 383–388.

Cavalcanti-Adam, E. A., Micoulet, A., Blümmel, J., Auernheimer, J., Kessler, H., & Spatz, J. P. (2006). Lateral spacing of integrin ligands influences cell spreading and focal adhesion assembly. European Journal of Cell Biology, 85(3–4), 219–224.

Chen, L., Xu, J., Holmes, J. D., & Morris, M. A. (2010). A facile route to ZnO nanoparticle superlattices. Synthesis, functionalization, and self-assembly. Journal of Physical Chemistry C, 114(5), 2003–2011.

El-Atwani, O., Aytun, T., Mutaf, O. F., Srot, V., van Aken, P. A., & Ow-Yang, C. W. (2010). Determining the morphology of polystyrene-block-poly(2-vinylpyridine) micellar reactors for ZnO nanoparticle synthesis. Langmuir, 26(10), 7431–7436.

Farzaneh, F., & Hamedani, N. F. (2006). Synthesis of ZnO nanocrystals with hexagonal (Wurtzite) structure in water using microwave irradiation. Journal of Sciences, Islamic Republic of Iran, 17(3). Retrieved July 11, 2012, from http.//journals.ut.ac.ir/page/article-frame.html?langId=en&articleId=1002741

Gao, X., Cui, Y., Levenson, R. M., Chung, L. W. K., & Nie, S. (2004). In vivo cancer targeting and imaging with semiconductor quantum dots. Nature Biotechnology, 22(8), 969–976.

Hines, M. A., & Guyot-Sionnest, P. (1996). Synthesis and characterization of strongly luminescing ZnS-capped CdSe nanocrystals. Journal of Physical Chemistry, 100(2), 468–471.

Kjærgaard, K., Sørensen, J. K., Schembri, M. A., & Klemm, P. (2000). Sequestration of zinc oxide by fimbrial designer chelators. Applied and Environmental Microbiology, 66(1), 10–14.

Matko, J., Bushkin, Y., Wei, T., & Edidin, M. (1994). Clustering of class I HLA molecules on the surfaces of activated and transformed human cells. Journal of Immunology, 152(7), 3353–3360.

Moffitt, M., & Eisenberg, A. (1995). Size control of nanoparticles in semiconductor- polymer composites. 1. Control via multiplet aggregation numbers in styrene-based random ionomers. Chemistry of Materials, 7(6), 1178–1184.

Murray, C. B., Norris, D. J., & Bawendi, M. G. (1993). Synthesis and characterization of nearly monodisperse CdE (E = sulfur, selenium, tellurium) semiconductor nanocrystallites. Journal of the American Chemical Society, 115(19), 8706–8715.

Nanda, J., Sapra, S., Sarma, D. D., Chandrasekharan, N., & Hodes, G. (2000). Size- selected zinc sulfide nanocrystallites. Synthesis, structure, and optical studies. Chemistry of Materials, 12(4), 1018–1024.

Nanotechnology Reviews, 6(4), 403-415. https.//doi.org/10.1515/ntrev-2017-0102

Qu, L., & Peng, X. (2002). Control of photoluminescence properties of CdSe nanocrystals in growth. Journal of the American Chemical Society, 124(9), 2049–2055.

Riley, J. (2018). Photoelectrochemistry of CdS multilayers. [Unpublished MSc Thesis]. University of Oxford.

Skaff, H., & Coughlin, E. B. (2002). Preparation of cadmium selenide-polyolefin composites from functional phosphine oxides and ruthenium-based metathesis. Journal of the American Chemical Society, 124, 5729.

Skaff, H., & Emrick, T. (2003). The use of 4-substituted pyridines to afford amphiphilic, pegylated cadmium selenide nanoparticles. Chemical Communications, 2003(1), 52– 53.

Smith, T. (2017). Dynamic light scattering in nanomaterial characterization.

Song, Z., Kelf, T. A., Sanchez, W. H., Roberts, M. S., Rička, J., Frenz, M., et al. (2011). Characterization of optical properties of ZnO nanoparticles for quantitative imaging of transdermal transport. Biomedical Optics Express, 2(12), 3321–3333.

Tomczak, N., Jańczewski, D., Han, M., & Vancso, G. J. (2009). Designer polymer– quantum dot architectures. Progress in Polymer Science, 34(5), 393–430.

Wang, X., Du, Y., Ding, S., Wang, Q., Xiong, G., & Xie, M., et al. (2006). Preparation and third-order optical nonlinearity of self-assembled chitosan/CdSe-ZnS core-shell

quantum dots multilayer films. Journal of Physical Chemistry B, 110(4), 1566–1570.

Wikipedia contributors. (2012). Quantum dot. Wikipedia, The Free Encyclopedia. Wikimedia Foundation, Inc. Retrieved September 2, 2012, from http.//en.wikipedia.org/w/index.php?title=Quantum_dot&oldid=508668703

Wiley InterScience.

Williams, K. A., & Hunt, H. D. (2015). The synthesis and applications of ZnO nanoparticles. Nanoscience and Nanotechnology Letters, 4(5), 348-360. https.//doi.org/10.1142/S1793292015500041

Wolfram, T., Belz, F., Schoen, T., & Spatz, J. (2007). Site-specific presentation of single recombinant proteins in defined nanoarrays. Biointerphases, 2(1), 44–48.

Wu, Z., Zhao, Y., Qiu, F., Li, Y., Wang, S., Yang, B., et al. (2009). Forming water- soluble CdSe/ZnS QDs using amphiphilic polymers, stearyl methacrylate/methylacrylate copolymers with different hydrophobic moiety ratios and their optical properties and stability. Colloids and Surfaces A. Physicochemical and Engineering Aspects, 350(1–3), 121–129.

Zhao, H., Douglas, E. P., Harrison, B. S., & Schanze, K. S. (2001). Preparation of CdS nanoparticles in salt-induced block copolymer micelles. Langmuir, 17(26), 8428–8433.

Zhou, M., & Ghosh, I. (2006). Quantum dots and peptides. A bright future together.